Applied Catalysis B: Environmental 87 (2009) 171–180

Contents lists available at ScienceDirect

Applied Catalysis B: Environmental

journal homepage: www.elsevier.com/locate/apcatb

Mesoporous silica–alumina as support for Pt and Pt–Mo sulfide catalysts: Effect of Pt loading on activity and selectivity in HDS and HDN of model compounds

Daniela Gulková [a], Yuji Yoshimura [b], Zdeněk Vít [a,*]

[a] Institute of Chemical Process Fundamentals of the AS CR, v. v. i., Rozvojová 135, 165 02 Prague 6, Czech Republic
[b] Research Center for New Fuels and Vehicle Technology, AIST, Tsukuba Central 5, 1-1-1 Higashi, Tsukuba 305-8565, Japan

ARTICLE INFO

Article history:
Received 11 June 2008
Received in revised form 8 September 2008
Accepted 10 September 2008
Available online 18 September 2008

Keywords:
Platinum
Molybdenum sulfide catalyst
MSA
Hydrodesulfurization
Hydrodenitrogenation

ABSTRACT

The potential of mesoporous silica–alumina (MSA) material as support for the preparation of sulfided Pt and Pt–Mo catalysts of varying Pt loadings was studied. The catalysts were characterized by their texture, hydrogen adsorption, transmission electron microscopy, temperature programmed reduction (TPR) and by activity in simultaneous hydrodesulfurization (HDS) of thiophene and hydrodenitrogenation (HDN) of pyridine. Sulfided Pt/MSA catalysts with 1.3 and 2 wt.% Pt showed almost the same HDS and higher HDN activities per weight amounts as conventional CoMo and NiMo/Al_2O_3, respectively. The addition of Pt to sulfided Mo/MSA led to promotion in HDS and HDN with an optimal promoter content close to 0.5 wt.%. The results of TPR showed strong positive effect of Pt on reducibility of the MoS_2 phase which obviously reflects in higher activity of the promoted catalysts. The activity of the MSA-supported Pt–Mo catalyst containing 0.5 wt.% Pt was significantly higher than the activity of alumina-supported Pt–Mo catalyst. Generally, Pt–Mo/MSA catalysts promoted by 0.3–2.3 wt.% Pt showed lower HDS and much higher HDN activities as compared to weight amounts of CoMo and NiMo/Al_2O_3. It is proposed that thiophene HDS and pyridine hydrogenation proceed over Pt/MSA and the majority of Pt–Mo/MSA catalysts on the same type of catalytic sites, which are associated with sulfided Pt and MoS_2 phases. On the contrary, piperidine hydrogenolysis takes place on different sites, most likely on metallic Pt fraction or sites created by abstraction of sulfur from MoS_2 in the presence of Pt.

1. Introduction

Platinum catalysts have often been studied from the point of view of hydrorefining in the last two decades. Sulfided Pt belongs to active noble metal sulfides of the 3rd row in hydrodesulfurization (HDS) of simple model compounds like dibenzothiophene (DBT) or thiophene [1,2] and to the most active ones in hydrodenitrogenation (HDN) [3]. Platinum also shows an excellent hydrogenating activity and it seems thus promising candidate for the deep HDS, where the hydrogenation (HYD) of aromatic ring preceding HDS makes transformation of the most refractory sulfur compounds easier [4–7]. Furthermore, a continuously increasing trend in hydrotreatment of heavier fractions containing greater amounts of nitrogen compounds, severely inhibiting HDS over conventional CoMo (NiMo) catalysts, requires more efficient catalysts also in HDN or those with properly balanced HDS and HDN activities.

Monometallic platinum catalysts, both sulfided and reduced, have mainly been studied in HDS of DBT, substituted BDT's [5–9], thiophene [10–13], and less often in HDN of quinoline [14] and pyridine [11]. These catalysts contained around 0.5–5 wt.% Pt and have most frequently been prepared from amorphous silica–alumina (ASA) [5–9], alumina [5–7,11,12], ZSM-5 and mesoporous carriers like Al-SBA-15 and MCM-41 [10,13]. Platinum has often been deposited on acidic carriers because it is widely accepted that their acidity increases the electron-deficient character of the Pt particles, which leads to the higher resistance to sulfur poisoning and better activity [6,7,15]. Moreover, Brønsted acidity of supports is also supposed to take part in thiophene HDS over Pt catalysts [10,13]. Platinum in smaller amounts has also been applied as a promoter of the Mo sulfide phase [9,11,12,16–19] and conventional CoMo, NiMo, NiW/Al_2O_3 catalysts [20]. The most often studied reactions were HDS [8,11,12,16,17,19–22], HYD [12,18–20] and HDN [11], and the most widely used carrier of the binary Pt–Mo systems was alumina. Promotional effects have often been observed in HDS, HYD and HDN [11,12,16,19].

Recently, we found that the addition of 0.5 wt.% Pt to a sulfided Mo/Al_2O_3 catalyst led to the interesting catalytic effects observed

* Corresponding author. Tel.: +420 220 390 284; fax: +420 220 920 661.
E-mail address: vit@icpf.cas.cz (Z. Vít).

0926-3373/$ – see front matter © 2008 Elsevier B.V. All rights reserved.
doi:10.1016/j.apcatb.2008.09.004

during simultaneous HDS of thiophene and HDN of pyridine [11] as well as in simultaneous HDS of thiophene and HYD of cyclohexene [12]. Synergetic effects around 1.6–2 were observed over this Pt–Mo(S)/Al_2O_3 catalyst in HDS and HYD and little stronger ones (2–4) in HDN. The HDS and HDN activities of the Pt–Mo(S)/Al_2O_3 catalyst were comparable with those achieved more recently over mesoporous SBA-15-supported Ni phosphide catalysts under the same experimental conditions [23]. The use of mesoporous solids based on silica and silica–alumina attracts increasing attention because of possible applications as acidic carriers of unique properties in different reactions, including hydrotreatment. In contrast to zeolites, their pores are larger, approaching several nanometers, which allows entering and more facile diffusion of bulky molecules. At the same time, their acidic strength is weaker, avoiding thus undesirable cracking and coking. Some of these materials like Al-doped SBA-15 [13,15] and Zr-doped SiO_2 [18] have recently been used for the preparation of Pt catalysts and studied in connection with hydrotreating. Similarly, a mesoporous silica–alumina (MSA) with disordered pore structure has recently been synthesized in our laboratory as carrier for Mo and noble metal catalysts [24]. This carrier showed a very narrow pore distribution with the mean pore diameter of 3.5 nm and also sufficient stability to thermal and water treatments. Our preceding work demonstrated suitability of this carrier for preparations of active Mo sulfide catalysts promoted by small amounts of Pt [25] and Rh [26].

The aim of this work was to evaluate in more detail the catalytic properties of MSA-supported Pt and promoted Pt–Mo sulfide systems. The main attention was paid to the effect of varying Pt loadings both in monometallic Pt and promoted Pt–Mo systems and the comparison of their activities and selectivities with their alumina-supported Pt and Pt–Mo counterparts and industrial CoMo and NiMo/Al_2O_3 catalysts. The test reaction was simultaneous HDS and HDN of simple model compounds, thiophene and pyridine, performed under low concentration of both reactants close to 200 ppm in the gas phase at 320 °C and 20 bar of overall pressure.

2. Experimental

2.1. Catalysts

MSA was synthesized from aqueous solutions of sodium metasilicate and aluminum nitrate by the procedure described in detail elsewhere [24]. The dried product was calcined in air at 500 °C for 6 h, crushed and sieved to the particle size of 0.16–0.315 mm. The MSA contained 50 wt.% alumina and 0.24 wt.% Na_2O. Its BET surface area was 491 m^2/g, total pore volume 0.61 cm^3/g and mean pore diameter 3.5 nm. The MSA sample used in this work was identical with the carrier described in Refs. [24–26]. Its acidity expressed by an activity index in the skeletal isomerization of cyclohexene was comparable with the acidity index of a commercial ASA [24].

The Pt/MSA catalysts were prepared by impregnation of the MSA (3 g) by appropriate amounts of ethanol solution of Pt acetylacetonate ($Pt(acac)_2$, 0.08 g in 58 ml) or aqueous solution of H_2PtCl_6 (0.08 g in 10 ml) at room temperature for 1 h, followed by evaporation of the solvent on a rotary evaporator under vacuum at 60 °C. Part of dried catalysts was reduced by H_2 at 400 °C for 1 h for determination of Pt dispersion. The remaining part of dried catalysts was directly sulfided by a mixture of 10% H_2S in H_2 at 400 °C for 1 h and stored under Ar/H_2 (95% Ar) for catalytic tests and temperature programmed reduction (TPR). The MoO_3/MSA catalyst was prepared by impregnation of the MSA by aqueous solution of ammonium heptamolybdate (AHM) keeping pH of the solution close to 9 by NH_4OH. A slurry of 18 g MSA and 30 ml H_2O was mixed at room temperature with solution of 6.5 g AHM in 60 ml H_2O and 8 ml 25% NH_4OH on a rotary evaporator. After 1 h, water was removed under vacuum at 80 °C and the product was dried at 150 °C for 2 h and calcined in air at 500 °C for 2 h. This procedure gave a well-dispersed MoO_3 phase [25]. The MoO_3/MSA was sulfided in a H_2S/H_2 mixture (10% H_2S) using temperature gradient 6 °C/min up to 400 °C and there keeping this temperature for 4 h. The average content of Mo in the sulfided catalyst determined from several analyses was 13 wt.% Mo. The promoted Pt–Mo/MSA catalysts were prepared by impregnation of the sulfided Mo/MSA by appropriate amounts of ethanol solution of $Pt(acac)_2$ or aqueous solution of H_2PtCl_6, similarly as in the case of Pt/MSA. In the case of H_2PtCl_6, pH of the slurry was close to 3. The dried promoted catalysts were sulfided by 10% H_2S in H_2 at 400 °C for 1 h and stored under Ar/H_2. The average content of Mo in the promoted catalysts was 12 wt.% Mo. The Pt and Pt–Mo catalysts are denoted by the symbols Pt(x)/MSA and Pt(y)Mo/MSA, where x, y mean wt.% of Pt. Industrial CoMo and NiMo/Al_2O_3 catalysts (S 344, 2.4 wt.% Co, 9.2 wt.% Mo and S 324, 2.8 wt.% Ni, 11.8 wt.% Mo, respectively) were included for comparison. They were sulfided by 10% H_2S in H_2 at 400 °C and stored under Ar/H_2.

2.2. Characterization

The contents of metals and sulfur were determined by inductively coupled plasma-atomic absorption spectroscopy (ICP/AAS) method. The contents of carbon and nitrogen in the spent catalysts were determined on a PerkinElmer Series II Analyser 2400. The surface areas were determined by a dynamic method using N_2 adsorption from N_2/He mixture on a FlowSorb III Instrument (Micromeritics). The BET surface areas and pore-size distributions of some selected samples were determined by N_2 adsorption on an ASAP2010M Instrument (Micromeritics) and calculated by the advanced BJH method from desorption branches of the isotherms. The samples were degassed at 400 °C in vacuum prior measurements.

The transmission electron microscopy (TEM) of the sulfided Pt–Mo/MSA catalyst was performed on a JEM-2000EX instrument (JEOL Hightech) using 200 kV accelerating voltage. The length and number of the MoS_2 slabs was evaluated from several images by measuring of about 250 stacks. The size of the Pt particles could only semi-quantitatively be estimated from observation of few visible Pt particles in the image of the promoted catalyst. The Pt dispersion in the reduced Pt/MSA catalyst was determined by pulse H_2 adsorption at 22 °C [27] and expressed as H/Pt ratio. The size of the Pt particles was calculated on adoption H/Pt = 1 stoichiometry according to Anderson and Pratt [28]. The sulfur coverage Θ_S of the Pt/MSA catalysts was calculated from H_2 uptakes at 22 °C as ratio $(n_R - n_S)/n_R$, where n_R and n_S are uptakes on the reduced and sulfided catalysts, respectively [29,30]. It was supposed that the size of Pt particles after reduction remains even after sulfidation [30].

The TPR of the catalysts was performed in a conventional apparatus by monitoring of hydrogen consumption by the thermal conductivity detector (TCD). Sulfided catalyst (0.2 g) was purged by He at 400 °C for 0.5 h in order to remove adsorbed H_2S and elemental sulfur and cooled to room temperature. Then the sample was heated to 950 °C by rate 5 °C/min in mixture 5 vol.% H_2 in Ar (35 ml/min). A column with molecular sieve Linde 13X was placed before the TCD in order to remove the evolved water and H_2S [31].

2.3. Catalytic tests

The activity in simultaneous HDS of thiophene and HDN of pyridine was evaluated in a flow fixed bed microreactor at

Table 1
Composition, sulfidation degree and surface areas of sulfided Pt, Mo and Pt–Mo/MSA catalysts.

Catalyst (carrier)	Composition (wt.%)			S/(Pt + Mo)	Surface area (m^2/g)
	Pt	Mo[a]	S		
MSA	0	0	0	–	444 (491)[b]
Pt(0.24)/MSA	0.24	0	–	–	448
Pt(0.52)/MSA	0.52	0	0.30	3.50	401
Pt(1.3)/MSA[c]	1.30	0	0.32	1.50 (0.72)[d]	414
Pt(2)/MSA[c]	2.00	0	0.44	1.34	413
Mo/MSA	0	13	8.7	1.93	270 (240)[b]
Pt(0.27)Mo/MSA	0.27	12	7.5	1.85	332
Pt(0.42)Mo/MSA	0.42	12	9.3	2.20	360 (257)[b]
Pt(0.5)Mo/MSA	0.50	12	8.0	1.93 (1.64)[d]	311
Pt(0.55)Mo/MSA[c]	0.55	12	9.4	2.30	310
Pt(1.2)Mo/MSA	1.20	12	6.4	1.81	277
Pt(2.3)Mo/MSA	2.30	12	7.0	1.73	196 (202)[b]

[a] Average value.
[b] BET value.
[c] Prepared from H_2PtCl_6.
[d] After reaction.

temperature 320 °C and overall pressure 20 bar, as described in detail elsewhere [11]. The catalyst amount (W) typically varied between 0.015 and 0.12 g. The feed generated by a pressure tension saturator contained 240 ppm of thiophene (TH) and 220 ppm of pyridine (PY) in the flow rate of H_2 150 ml/min. Before tests, catalysts were in situ reactivated by sulfidation in H_2S/H_2 mixture at atmospheric pressure under heating to 400 °C (rate of 6 °C/min) and there keeping at this temperature for 1 h. H_2S was then switched off and temperature of the catalyst was decreased to 320 °C in a stream of H_2. After reaching the reaction temperature, H_2 was replaced by the feed of the overall pressure 20 bar by a switching six-port valve. The samples of the feed and reaction mixture were taken automatically every 30 min with the sampling valco. The steady state was usually achieved after 4 h on stream, and the average composition of the reaction mixture was calculated from several subsequent analyses of the feed and reaction products. The on-line analyses were performed on a gas chromatograph HP 5890 equipped with FID detector and 3.5 m glass column packed with Carbopack B 60/80 4% Carbowax 20M (Supelco) and operating at 125 °C. The rate of the feed (F) was kept constant and the space time W/F was changed by the catalyst amount. Experiments at different W/F were always performed with the fresh catalyst charges. The integral dependences of the molar fractions of the components (a_i) on space time W/F were obtained for each catalyst. A blank experiment confirmed that under the experimental conditions used the MSA carrier alone was inactive.

The products of thiophene HDS were only C_4 hydrocarbons and H_2S. In HDN of PY, in addition to C_5 hydrocarbons and NH_3, also appreciable amounts (6–26%) of intermediate piperidine (PIP), were found. The HDN was described for simplicity by two irreversible consecutive steps, i.e., PY hydrogenation and PIP hydrogenolysis. Both HDS and HDN were described by pseudo-first order kinetic equations derived elsewhere [12,27]. The activities of the catalysts were expressed by the rate constants for thiophene HDS (k_{TH}), PY hydrogenation (k_{PY}) and PIP hydrogenolysis (k_{C5}). The rate constants were calculated by non-linear regression from the dependences $a_i = f(W/F)$. The overall HDN activity A(HDN) was defined as the reciprocal value of W/F, at which the PY conversion into C_5 hydrocarbons achieved 0.5 [11]. This is a simple index of HDN activity useful for direct comparison of catalysts, because neither k_{PY} nor k_{C5} alone gives information about the overall HDN activity. The HDN/HDS selectivity ($S_{HDN/HDS}$) was defined by the value of a_{C5} achieved when the molar fraction of thiophene approached 0.5.

3. Results and discussion

3.1. Properties of catalysts

The contents of metals and sulfur, sulfidation degree and surface areas of the prepared catalysts are listed in Table 1. For easy comparison of promotional effect, monometallic Pt/MSA and promoted Pt–Mo/MSA catalysts were prepared with the aim to have approximately the same Pt loadings per mass unit in these catalysts. The ICP analyses confirmed that this goal was achieved. Both $Pt(acac)_2$ and H_2PtCl_6 were used to deposit Pt in the case of monometallic as well as promoted catalysts. However, the use of H_2PtCl_6 as a precursor is simpler and moreover, it allows to achieve the required Pt loading with the higher accuracy. This is probably given by the much stronger adsorption of H_2PtCl_6 on MSA compared to $Pt(acac)_2$. As far as the sulfidation degree of Pt in the Pt/MSA is concerned, the S/Pt ratio exceeding 1 suggests that a part of sulfur is present in elemental form. The ratios S/(Pt + Mo) in freshly sulfided Mo and Pt–Mo/MSA catalysts were close to 2, which confirms that the MoS_2 phase is sufficiently sulfided.

Deposition of low amounts of Pt on the MSA led to only small decrease of surface areas of the catalysts (Table 1). On the other hand, deposition of large amount of the Mo phase caused a substantial decrease of the surface to about 60% of the original value. The subsequent modification of the sulfided Mo/MSA by small amounts of Pt led to an interesting effect. Instead of gradual and small decrease, analogous to that observed for Pt/MSA, the surface areas of the catalysts modified by about 0.3–0.6 wt.% Pt again increased, giving a distinct maximum at around 0.4 wt.% Pt. This was verified by the pore size distributions of the Pt/MSA and Pt(0.42)Mo/MSA, although the observed difference was smaller than in the case of dynamic method. These changes of the surface areas are very similar to those observed recently by other authors during preparation of Pt–MoO_3/ASA and Pt–MoO_3/Al_2O_3 catalysts [9,17]. The increase of surface area of the oxidic MoO_3/ASA catalyst after deposition of 1% Pt was explained by redispersion of the MoO_3 phase [9]. Recently, it has been shown that the reduction of unsupported MoO_3 by hydrogen in the presence of Pt proceeds via formation of nonstoichiometric compound H_xMoO_3 which is accompanied by the marked increase of MoO_3 surface area up to 250 m^2/g [32]. It is also known that MoS_2 adsorbs hydrogen to give the analogous compound H_xMoS_2 [33,34] and that hydrogen uptake on MoS_2 increases in the presence of Pt [35]. All these facts led us to assume that the observed increase in surface areas of our

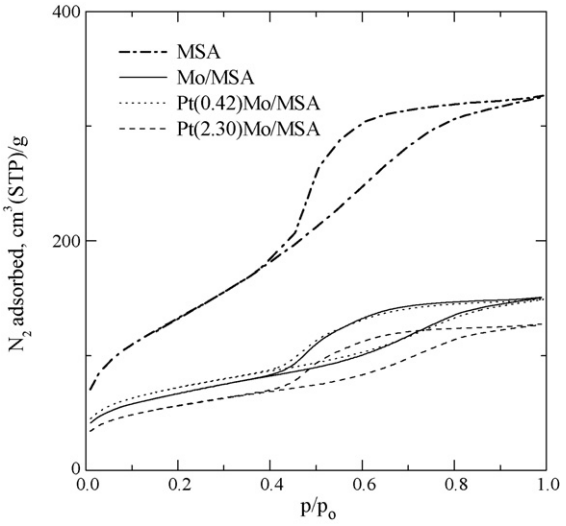

Fig. 1. Adsorption isotherms of MSA, sulfided Mo/MSA, Pt(0.42)Mo/MSA and Pt(2.3)Mo/MSA catalysts.

Pt–Mo/MSA catalysts could be caused by the formation of H_xMoS_2 compounds during sulfidation of the promoted catalysts. The conditions of sulfidation are convenient for such a process because of the reducing atmosphere, presence of Pt and the temperature range up to 400 °C.

Fig. 1 shows nitrogen adsorption isotherms for the MSA carrier, sulfided Mo/MSA and two samples promoted by 0.42 and 2.3 wt.% Pt. It is seen that mesoporous character of the catalysts remains well preserved even after depositions of Mo and at the highest Pt loading. The adsorbed nitrogen amounts and BET surface areas of these samples complement well the values obtained by dynamic sorption (Table 1). The pore size distributions of the catalysts remain very narrow with maxima close to the maximum of the parent MSA, which demonstrates that the uniformity of the pores was also preserved in the prepared catalysts (Fig. 2). However, this behavior suggests that deposition of Mo led to plugging of some fraction of the pores. The total pore volume of the Mo/MSA and of both promoted catalysts decreased to about 0.23 cm^3/g, in comparison to the value of 0.61 cm^3/g for the parent MSA.

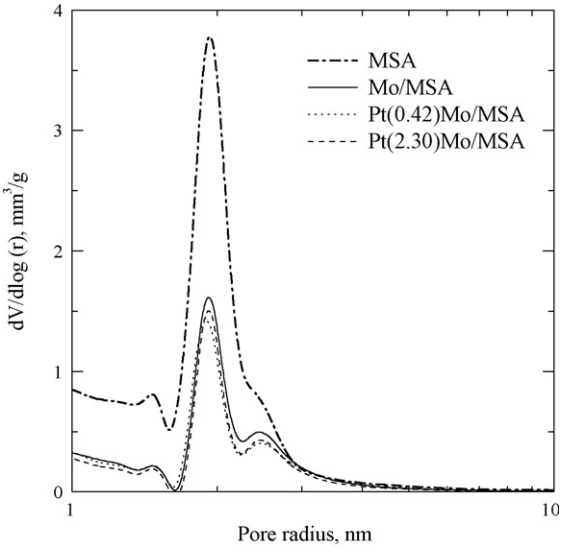

Fig. 2. Pore size distributions of MSA, sulfided Mo/MSA, Pt(0.42)Mo/MSA and Pt(2.3)Mo/MSA catalysts.

Table 2
Composition, Pt dispersion and sulfur coverage of monometallic Pt/MSA catalysts.

Catalyst	Pt loading (wt.%)	H/Pt[a]	d_{mean} (nm)	Θ_s[b]
Pt(0.24)/MSA	0.24	1.13	1.0	–
Pt(0.52)/MSA	0.52	0.87	1.3	1.00
Pt(1.3)/MSA[c]	1.30	0.64	1.8	1.00 (0.99)[d]
Pt(2)/MSA[c]	2.00	0.29	4.0	–

[a] After reduction.
[b] After sulfidation.
[c] Prepared from H_2PtCl_6.
[d] After reaction.

The reduced Pt/MSA catalysts show high H/Pt ratios close to 1 at the lowest Pt loadings that decrease when the loading approaches 2 wt.% Pt (Table 2). These values are similar to those obtained by Williams et al. for 0.8 wt.% Pt on ASA of a comparable composition (53% Al_2O_3) [36]. The H/Pt values obtained in the present work confirm a good Pt dispersion, at least for the loadings to around 1 wt.% Pt. The size of the Pt particles calculated from H_2 uptake is between 1 and 4 nm. Hydrogen sorption on two freshly sulfided Pt(0.52)/MSA and Pt(1.3)/MSA catalysts was completely suppressed which speaks for the quantitative coverage of Pt particles by sulfur. This finding is in a good agreement with studies of CO adsorption, which demonstrated that the coverage of well dispersed Pt particles by sulfur in sulfided Pt/ASA catalysts was quantitative [6,8] or close to 95% [30]. In order to obtain information about the state of Pt in the catalysts after reaction, the Pt(1.3)/MSA catalyst was examined again after 6 h run by H_2 sorption for sulfur coverage and by ICP analysis for sulfur content. Before both analyses, the sample was treated in hydrogen at 400 °C/1 h in order to remove adsorbed H_2S and elemental sulfur. So treated sample showed a very small H_2 uptake corresponding to 1% of the surface Pt atoms in the metallic state (Θ_S = 0.99, Table 2). This value is in a fairly good agreement with the atomic ratio S/Pt = 0.72 calculated from ICP analysis (Table 1). This S/Pt ratio is almost identical with that for accessible fraction of the metallic sites on reduced catalyst (H/Pt = 0.64, Table 2), showing clearly that sulfur content in the spent Pt(1.3)/MSA is still high enough to cover practically all accessible Pt sites.

Hydrogen adsorption cannot be used for reliable determination of the Pt dispersion in the promoted Pt–Mo/MSA catalysts. This is because of the presence of sulfur in the original sulfided Mo/MSA, that could poison the metallic Pt sites and moreover, due to the fact that MoS_2 alone is able to adsorb hydrogen, especially in the presence of Pt [35]. In this respect, some semi-quantitative information concerning the Pt dispersion in the promoted catalysts was obtained by TEM. The measurement of the sulfided Pt(0.5)Mo/MSA showed that the majority of visible MoS_2 particles contained 1–3 layers and small portion of multilayered structures (4 and 5 layers), and large MoS_2 crystallites were absent (Fig. 3a). The average length (L) of MoS_2 crystallites was 3.7 nm and the average number of layers (N) 1.8. Although these values differ to some extent from those reported recently by us for the parent Mo/MSA with L = 2.9 and N = 2.5 [25], they still confirm that the MoS_2 phase is well dispersed in both catalysts. The somewhat lower value N in the promoted catalyst indicates the lower degree of stacking and suggests a slightly better MoS_2 dispersion. It seems likely that this fact partly contributes to the higher activity of the promoted catalyst. On the other hand, the present data do not allow conclude whether this smaller difference is in any relation to an assumed presence of H_xMoS_2 phase in the promoted catalysts. Fig. 3b shows the selected area of the image of Pt(0.5)Mo/MSA catalyst in larger magnification. The discrete Pt particles were not observed, which could suggest a good Pt dispersion in the promoted catalyst. However, the closer inspection revealed few

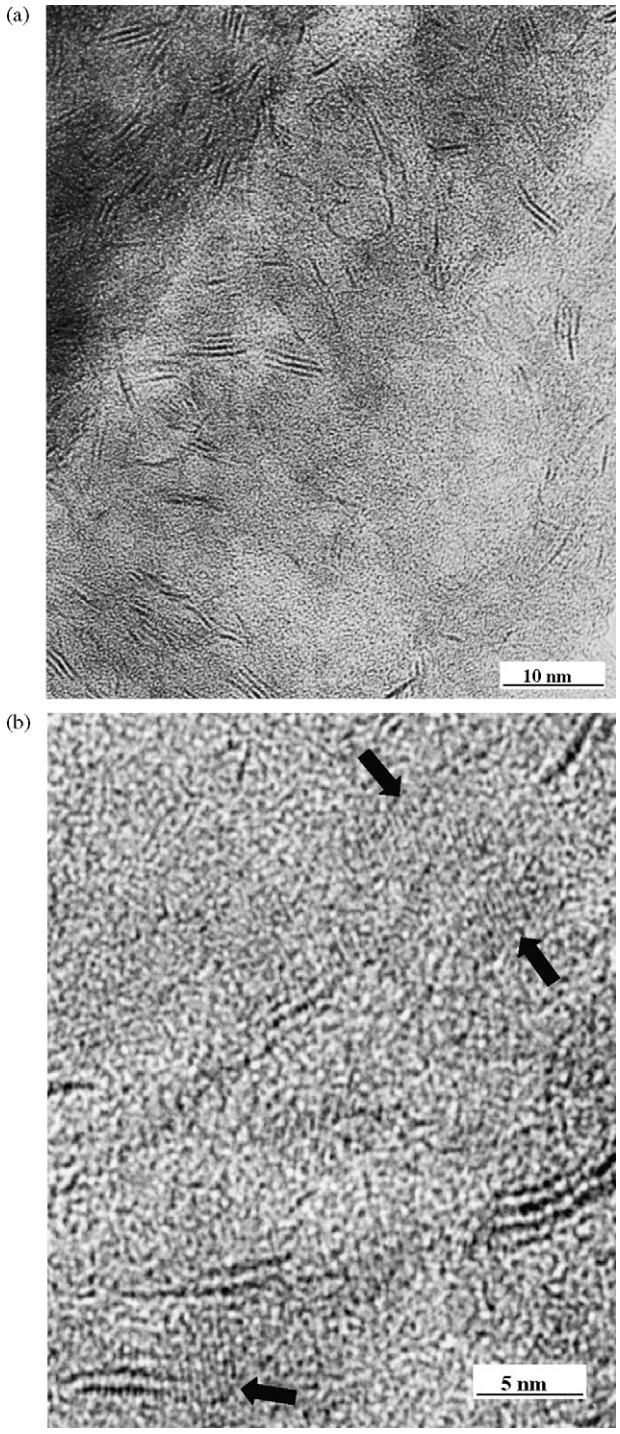

Fig. 3. TEM images of the sulfided Pt(0.5)Mo/MSA catalyst.

regions of the size 5–10 nm with regular fringe structure, marked in Fig. 3b by arrows. After the image processing (contrast, magnification), the distance between fringes was estimated to be around 0.272 nm which closely approaches the reference value of 0.277 nm corresponding to the metallic Pt^0(1 1 0) plane [37]. We therefore believe, that metallic phase is dominant for Pt particles of the size 5–10 nm in the freshly sulfided Pt–Mo/MSA catalyst. This conclusion seems to agree with the results reported by Navarro et al. who found only metallic Pt in the sulfided PtMo/ASA by XPS [9]. It is also probable, that for the larger Pt particles over 5 nm, the

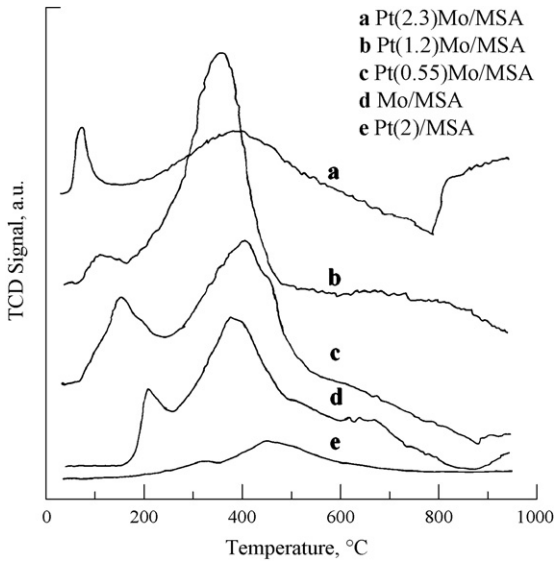

Fig. 4. TPR pattern of sulfided Pt, Mo and Pt–Mo/MSA catalysts. The curves are shifted for clarity and correspond to the same catalyst weight.

bulk metal structure substantially remains even after sulfidation, which proceeds mainly on their surface [38].

The TPR pattern of sulfided Pt, Mo and selected Pt–Mo/MSA catalysts are shown in Fig. 4. The Pt(2)/MSA catalyst showed a maximum at 465 °C, analogous to maxima between 400 and 500 °C found by other authors on sulfided Pt/Al_2O_3 catalysts, which were ascribed to the reduction of PtS [39,40]. The Mo/MSA sample displayed two maxima, similarly as sulfided Mo/Al_2O_3 [31,39]. The first maximum in the low temperature region close to 200 °C was ascribed by Mangnus et al. to reduction of nonstoichiometric sulfur species S_x [39]. The pattern of the promoted Pt–Mo/MSA catalysts were different from that corresponding to Mo/MSA. The most significant changes were shift of the first maximum (T^1_{max}) to much lower temperatures and changing areas under the TPR curves. These areas correspond to hydrogen consumption during TPR which is proportional to amounts of reducible sulfur species. The TPR areas were evaluated for the range 25–400 °C, i.e., up to maximum temperature used during catalysts activation. These areas are summarized, together with temperature maxima, in Table 3.

Fig. 4 shows that addition of Pt to Mo/MSA up to 2.3 wt.% caused significant decrease of T^1_{max}. In contrast to monometallic catalysts, reduction of the promoted catalysts started already at temperatures below 100 °C. It should be emphasized that this process cannot involve reduction of elemental sulfur, because it was removed by purging of the samples by He at 400 °C before TPR, similarly as in Refs. [31,39]. The low temperature peak could exclusively be ascribed to reduction of strongly bonded, but easily reducible sulfur atoms, most likely associated with the MoS_2 phase. Moreover, data in Table 3 show that also the amounts of

Table 3
Temperature maxima and TPR areas for sulfided Mo, Pt–Mo and Pt/MSA catalysts.

Catalyst	T^1_{max} (°C)	T^2_{max} (°C)	Area[a] (a.u.)
Mo/MSA	210	395	1.00
Pt(0.55)Mo/MSA[b]	150	408	1.27
Pt(1.2)Mo/MSA	95	382	1.54
Pt(2.3)Mo/MSA	75	400	0.55
Pt(2)/MSA[b]	465	–	0.13

[a] For the range 25–400 °C, normalized to the same catalyst weight.
[b] Prepared from H_2PtCl_6.

reducible sulfur species increased up to 1.2 wt.% Pt. The highest Pt loading in Pt(2.3)Mo/MSA led to an additional interaction, most likely reduction of bulk MoS_2 above 800 °C, while reduction between 250 and 550 °C was limited. The effect of Pt on reducibility of the MSA-supported MoS_2 phase was very strong. About 1 wt.% Pt caused decrease of T^1_{max} by more than 100 °C and, at the same time, increased the amount of reducible sulfur species by one half. It is worth to mention, that theoretical contribution corresponding to the reduction of the equivalent of the PtS phase in Pt(1.2)Mo/MSA should lead to only 8% increase of TPR area, instead of the observed 54%. This confirms that sulfided Pt and MoS_2 in the promoted catalysts do not behave as independent phases showing only additive behavior. In general, character of all these pattern suggests that both the quality and amounts of the reducible sulfur species of MoS_2 were greatly influenced by Pt addition.

3.2. Activity of catalysts

The activity of monometallic Pt and promoted Pt–Mo/MSA catalysts was almost constant during catalytic tests and only small deactivation was observed. In contrast, the activity of Mo/MSA catalyst significantly diminished during the first 2–3 h on stream, as shown in Fig. 5. The elemental analyses of the spent Mo/MSA and Pt–Mo/MSA catalysts after 6 h runs revealed that the former catalyst contained 4.55 wt.% C and 1.03 wt.% N, i.e., almost twofold amount compared to the Pt(1.2)Mo/MSA having 2.36 wt.% C and 0.58 wt.% N. In both cases, the atomic C/N ratios were close to 5, speaking for the presence of strongly adsorbed pyridine or possibly some condensation products. Pyridine could be adsorbed both on Brønsted and Al^{3+} sites of the support. The C/N ratio was slightly higher for Mo/MSA (5.15) and lower for Pt(1.2)Mo/MSA (4.75), which can be due to the presence of coke in the non-promoted catalyst. The higher deposits and C/N ratios explain the stronger deactivation of the parent Mo/MSA catalyst. Platinum probably facilitates transformation of pyridine or carbonaceous deposits into volatile reaction products and contributes to the restoration of the free catalyst surface.

Fig. 6 shows the steady state composition of the reaction products as a function of contact time over Pt(0.5)Mo/MSA. Similar dependences were obtained for all the catalysts and used for evaluation of their activity and selectivity. The rate constants of

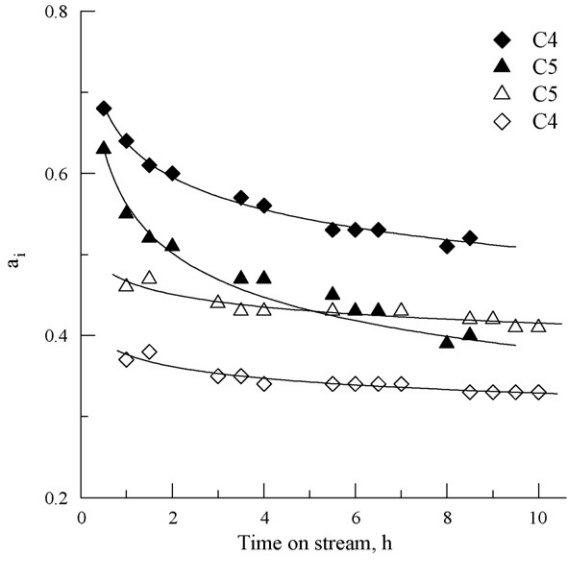

Fig. 5. Conversion in C_4 and C_5 hydrocarbons as function of time on stream. Catalyst weight: 0.121 g Mo/MSA (full points) or 0.016 g Pt(1.2)Mo/MSA (open points).

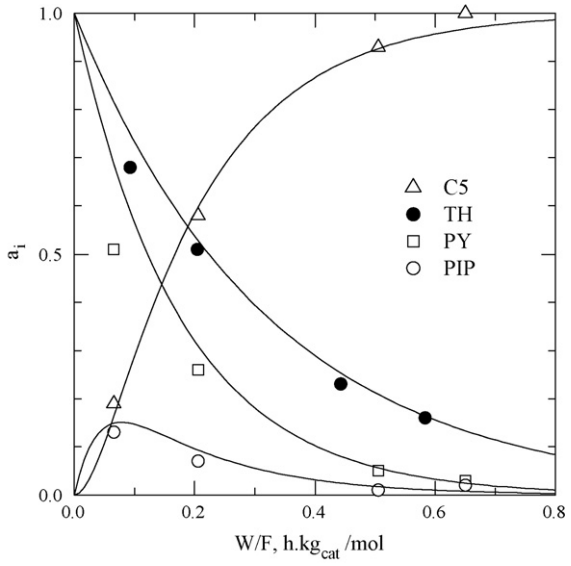

Fig. 6. Composition of reaction products as a function of space time over Pt(0.5)Mo/MSA catalyst.

thiophene HDS (k_{TH}), pyridine HYD (k_{HY}) and piperidine hydrogenolysis (k_{C5}) as well as the values A(HDN) and HDN/HDS selectivities are summarized in Table 4. The data show that the addition of Pt to the Mo/MSA leads to substantial enhancement of the activities in HDS and HDN and, that the activities of both monometallic and promoted Pt–Mo/MSA catalysts increased steadily with increasing Pt loading. The increment of the activity of the promoted catalysts was remarkably fast to about 0.5 wt.% Pt and then became much less pronounced. Such a sudden change-over is caused by markedly higher surface areas of the catalysts promoted by 0.3–0.6 wt.% Pt. The HDS activities of the promoted Pt–Mo/MSA catalysts exceed the activity of the Mo/MSA but remain below that of the monometallic Pt/MSA. The same order of the activities in HDS of DBT has been observed by Navarro et al. over ASA-supported Pt and Pt–Mo catalysts [9] and Y zeolite-supported Pd and Pd–Mo catalysts [41]. In the latter case, the lower HDS activity of the promoted Pd–Mo/Y catalysts than Pd/Y one was ascribed to the inhibition of HDS by H_xMoS_2 [41].

In order to eliminate the effect of varying surface areas of the promoted catalysts, the rate constants were further normalized to unit surface area. This allows gaining a more straightforward insight into the role of the amount of Pt added. Fig. 7 shows the dependences of the activities of Pt/MSA catalysts plotted against surface Pt atom density. The normalized rate constants k_{TH} and k_{PY} increase more or less linearly with increasing density of Pt atoms over the whole concentration range. On the contrary, the k_{C5} values attained relatively high values already at the lowest Pt loading and then change only negligibly. A clear parallelism between k_{PY} and k_{TH} on one side and different dependence of k_{C5} on the amount of added Pt on the other side suggest that thiophene HDS and pyridine HYD proceed on the same type of sites which are different from those taking part in the C–N bond hydrogenolysis. From the linearity of data in Fig. 7 one can further deduce that HDS and pyridine HYD proceed well also on larger Pt clusters present at Pt loadings around 2 wt.%, i.e., that both reactions are not sensitive to decreasing Pt dispersion, which is indicated by data in Table 2. We assume that both reactions proceed on sites present on sulfided Pt phase. On the other hand, the plateau in the k_{C5} values established already at low Pt contents demonstrates the sensitivity of the C–N bond hydrogenolysis to Pt dispersion. We therefore conclude that this step proceeds on different sites located most likely on the

Table 4
Activity and selectivity in simultaneous HDS of thiophene and HDN of pyridine at 320 °C and 20 bar.

Catalyst	k_{TH} (mol/h·kg$_{cat}$)	k_{PY} (mol/h·kg$_{cat}$)	k_{C5} (mol/h·kg$_{cat}$)	A(HDN) (mol$_{C5}$/h·kg$_{cat}$)	$S_{HDN/HDS}$
Mo/MSA	0.7	1.2	1.9	1.0	0.41
Pt(0.24)/MSA	0.6	0.7	0.5	0.4	0.15
Pt(0.52)/MSA	1.4	1.4	3.5	1.2	0.29
Pt(1.3)/MSA[a]	4.1	3.7	3.2	2.1	0.12
Pt(2)/MSA[a]	7.4	5.1	4.7	2.9	0.07
Pt(0.27)Mo/MSA	1.5	3.4	7.5	2.9	0.65
Pt(0.42)Mo/MSA	1.9	3.6	20.0	4.3	0.69
Pt(0.5)Mo/MSA	3.1	5.7	24.2	6.0	0.64
Pt(0.55)Mo/MSA[a]	3.1	6.1	23.3	6.3	0.66
Pt(1.2)Mo/MSA	2.7	6.0	25.6	6.3	0.72
Pt(2.3)Mo/MSA	3.6	9.2	28.1	8.3	0.75
$CoMo/Al_2O_3$	4.3	1.9	1.8	1.1	0.03
$NiMo/Al_2O_3$	8.1	2.5	6.1	2.2	0.04

[a] Prepared from H_2PtCl_6.

corners and edges of Pt crystallites and associated with the metallic Pt fraction. Both kinds of sites coexist in sulfided Pt catalysts. Their amounts depend on the ratio PtS/Pt, which is influenced by conditions of sulfidation or activation [40] and partial pressures of H_2S and H_2 [30]. The high Θ_S values of the fresh and spent Pt(1.3)/MSA catalyst speak in favor of possibility, that during reaction majority of Pt atoms of Pt/MSA catalyst was covered by sulfur. We therefore conclude that majority of active sites of our sulfided Pt/MSA catalysts are associated with sulfided Pt phase dominating over small fraction of the metallic sites.

The dependences of the normalized activities of the promoted Pt–Mo/MSA catalysts on surface Pt atom density are shown in Fig. 8. The k_{C5} and k_{PY} values are substantially higher than those for the monometallic Pt/MSA catalysts, which is given by the strong promotion in HDN and will be discussed later. It is interesting that the dependence for k_{C5} is again clearly non-linear while k_{PY} and k_{TH} dependences (except for two points at 0.5 and 0.55 wt.% Pt) can be considered as well linear. This result suggests that also in this case HDS and pyridine HYD proceed on the same type of active sites different from those active in C–N bond hydrogenolysis. The promoted catalysts behave therefore in the same manner as the Pt/MSA, but their activities are different. It seems that activity of sulfided Pt phase is strengthened by the presence of the MoS_2, which suggests that the same type of sites is preserved, at least partly, in the promoted Pt–Mo/MSA catalysts.

The activity of the promoted catalysts in HDS of thiophene and HDN of pyridine shows obviously complex character. It can be expected that some parts of sulfided Pt and MoS_2 phases keep their own catalytic properties, behaving as individual components and contributing in this way to overall activity. Besides this, some parts of both phases obviously strongly influence each other, either due to closer contact or through to migration of activated hydrogen. The results obtained by TPR confirmed the strong effect of Pt addition on reducibility of MoS_2 phase already at relatively low temperatures. Such reduction undoubtedly takes part also during reaction at 320 °C and higher hydrogen pressure and leads to partial removal of reactive sulfur atoms of MoS_2. This is in line with the observed lower ratio S/(Pt + Mo) = 1.64 found in the used Pt(0.5)Mo/MSA catalyst after 6 h catalytic run (Table 1). Higher degree of reduction of the MoS_2, induced by addition of Pt, can reflect in higher intrinsic activity of the MoS_2 phase. The distinctly higher k_{TH} and k_{PY} values for two samples promoted by 0.5 and 0.55 wt.% Pt shown in Fig. 8 could be in relation to different quality of sites that might be related to the presence of H_xMoS_2. Such hypothesis is in line with the considerations predicting its positive effect on the activity of the MoS_2 phase in reactions consuming

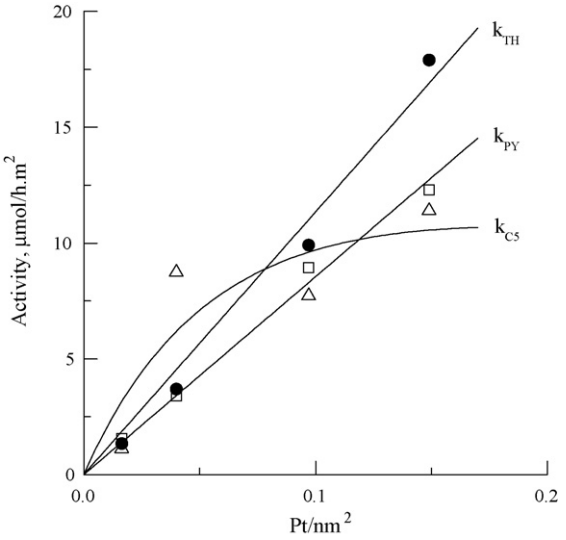

Fig. 7. Effect of surface Pt atom density on normalized rate constants k_{TH}, k_{PY} and k_{C5} for Pt/MSA catalysts.

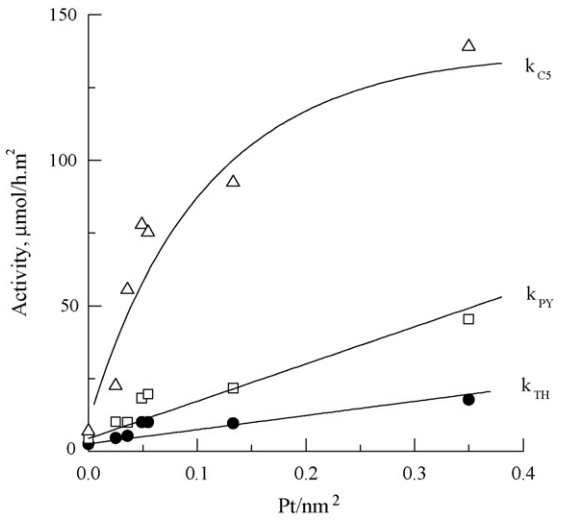

Fig. 8. Effect of surface Pt atom density on normalized rate constants k_{TH}, k_{PY} and k_{C5} for promoted Pt–Mo/MSA catalysts.

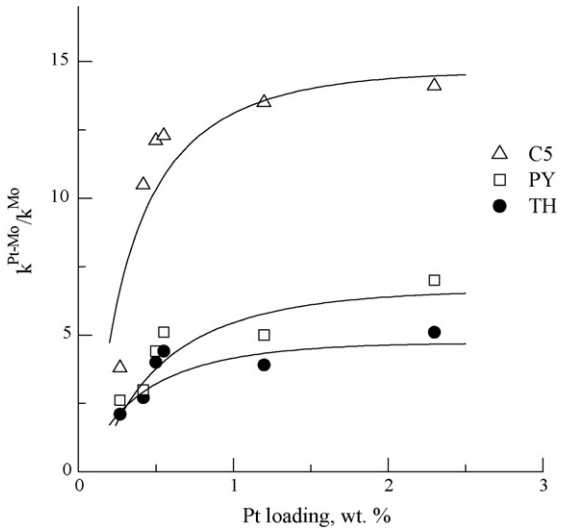

Fig. 9. Promotion as a function of Pt loading.

hydrogen [34]. Both HYD of pyridine and HDS of thiophene are indeed such cases. On the other hand, MoS_2 absorbs hydrogen at higher temperatures, especially in the presence of Pt [35]. One can therefore speculate, that a fairly large amount of MoS_2 in the catalyst can serve as a reservoir of hydrogen which is donated to active sites of the Pt sulfide phase. Such hypothesis could help to understand the observed similarity in activity trends of Pt/MSA and Pt–Mo/MSA catalysts. Very high C–N bond hydrogenolysis activity of the promoted catalysts apparent from data in Table 4 is probably connected, as we believe, with metallic character of sites, in particular with those created by deeper abstraction of sulfur atoms from MoS_2 phase in the presence of Pt particles and also possibly, in lesser extent, by residual fraction of the metallic Pt atoms. Moreover, this reaction step is also positively influenced by acidity of the MSA support, as was shown in the case of Mo and Rh–Mo catalysts [26].

3.3. Synergetic effect and HDN/HDS selectivity

The magnitude of promotion (P) for thiophene HDS, pyridine HYD and C–N bond hydrogenolysis was expressed by the ratio of the rate constants of the promoted (k^{Pt-Mo}) to Mo catalyst (k^{Mo}), based on the weight amounts of the catalysts. The P values as a function of Pt loading are shown in Fig. 9. It is seen that the addition of the smaller Pt amounts to Mo/MSA led to multiple activity increase in both reactions. This was very fast to about 0.5 wt.% Pt and then became slower. It is also apparent that the promotion was very strong in HDN and rather week in HDS. It seems that the most efficient promoter amount is around 0.5 wt.% Pt; further increase in Pt loading leads only to a minor effect. Fig. 9 shows that the use of $Pt(acac)_2$ and H_2PtCl_6 as precursors for Pt(0.5)Mo/MSA and Pt(0.55)Mo/MSA catalysts, respectively, gives the same P values. Both precursors show the same effectiveness, as already documented by almost identical activities of these catalysts.

Addition of Pt to Mo/MSA greatly influences HDN/HDS selectivity of the catalysts ($S_{HDN/HDS}$). Majority of the Pt/MSA catalysts, with the only exception of Pt(0.52)/MSA, show rather low C–N bond hydrogenolytic activity which reflects in the selectivities lower than that of Mo/MSA (Table 4). On the other hand, the promoted Pt–Mo/MSA catalysts possess much higher selectivity which exceeds markedly the values for the both monometallic systems. This is given by the strong promotion in the C–N bond hydrogenolysis and the weaker in pyridine HYD and thiophene HDS. A nice example of the shift of the selectivity accompanying the promotion is apparent from the data in Table 4. The $S_{HDN/HDS}$ values of all the promoted catalysts do not lie between the values for the monometallic Pt/MSA and Mo/MSA, but clearly out and far from this range. The exceptionally high $S_{HDN/HDS}$ values of the promoted Pt–Mo/MSA catalysts exceed the value for Pt–Mo(S)/Al_2O_3 [11].

3.4. Comparison of MSA- and alumina-supported Pt and Pt–Mo catalysts

MSA differs from Al_2O_3 in two respects. First, it possesses Brønsted acidity comparable to commercial ASA and capable of isomerization reactions, while Al_2O_3 not [24] and secondly, it has approximately twofold surface area over Al_2O_3, allowing the better dispersion of active components. Table 5 shows comparison of the specific activities of MSA- and alumina-supported monometallic Pt sulfide catalysts of similar loadings. It is seen that all the values of the specific activities of Pt/MSA are approximately fivefold those of Pt/Al_2O_3. However, these values are in fact influenced by different Pt dispersion, which is lower for Pt/Al_2O_3 (H/Pt = 0.38, Ref. [11]) than for Pt/MSA (H/Pt = 1.13). Nevertheless, taking into account these differences and calculating the specific activities per accessible site, the values for Pt/MSA are still by 35–80% higher than those for Pt/Al_2O_3. We ascribe this difference to the higher acidity of MSA. Such conclusion agrees well with recent literature data. The higher activities of ASA-supported Pt catalysts over alumina-supported ones, both sulfided and reduced, have been reported for HDS of DBT, substituted DBT's [5–7] and HDN of quinoline [14]. High hydrogenation and HDS activities of Pt/ASA are usually related to the ease of the creation of sulfur vacancies on small Pt particles, which is positively affected by acidity of carrier [6,7].

Because of the larger surface area and a relatively high Al_2O_3 content, the MSA can load the larger amount of well dispersed MoS_2 than conventional alumina. So, the Pt–Mo/MSA catalyst contains about 12 wt.% Mo in comparison to only 9 wt.% Mo in the Pt–Mo(S)/Al_2O_3 [11], which naturally reflects in the higher activity per weight unit of the MSA-supported catalyst. Table 5 gives the activities of these two catalysts normalized per mol of metals and shows that HDS activity of the MSA-supported catalyst is still by about 25% higher than that of the alumina-supported one and the difference is even higher in HDN. The use of MSA brings substantial

Table 5
Specific activity of MSA- and alumina-supported Pt and Pt–Mo catalysts. Simultaneous HDS of thiophene and HDN of pyridine at 320 °C and 20 bar.

Catalyst	Loading (wt.%)		k_{TH} (mol/h $mol_{(Pt+Mo)}$)	k_{PY} (mol/h $mol_{(Pt+Mo)}$)	k_{C5} (mol/h $mol_{(Pt+Mo)}$)
	Pt	Mo			
Pt(0.24)/MSA	0.24	0	49.0	57.0	41.0
Pt/Al_2O_3[a]	0.30	0	9.1	14.3	8.4
Pt(0.5)Mo/MSA	0.50	12	2.4	4.5	19.0
Pt–Mo(S)/Al_2O_3[a]	0.52	9	1.9	3.8	5.6

[a] Calculated from data in Ref. [11].

improvement of HDN of the promoted catalysts. This can be ascribed to the positive effect of Brønsted acidity making the C–N bond cleavage of intermediate PIP easier [26].

Difference between the normalized HDS activities of Pt–Mo/MSA and Pt–Mo/Al_2O_3 is smaller than that observed for the monometallic Pt catalysts (Table 5). We ascribe this result to the levelling effect of the MoS_2 phase. This conclusion is supported by our recent work that showed that the monometallic Mo/MSA possessed the lower thiophene HDS activity than Mo/Al_2O_3 at the same experimental conditions [26]. Blanchard et al. [15] observed that HDS of DBT was strongly accelerated by the increasing number of strongly acidic sites of Mo/BEA zeolite catalysts while this effect has not been found with NiMo/Al-SBA-15 catalysts. This different behavior was explained by the lower acid strength of Al-SBA-15 as compared to BEA. Similarly, in our case one can speculate that the absence of the positive effect of acidity in the case of monometallic Mo/MSA and Mo/Al_2O_3 catalysts can be related to the lower acid strength of MSA as compared to BEA zeolite, not allowing to increase sufficiently the catalytic properties of the MoS_2 phase, but still sufficient to do this with the Pt sulfide phase. The positive effect of acidity on thiophene HDS is then smaller for promoted Pt–Mo/MSA than for Pt/MSA catalysts.

3.5. Comparison with conventional catalysts

Thiophene HDS activities of monometallic Pt(1.3)/MSA and Pt(2)/MSA samples are per weight unit almost the same as the values for conventional CoMo and NiMo/Al_2O_3 catalysts (Table 4). High HDS activity of the Pt/MSA is in general agreement with recent observations of other authors. Sulfided ASA-supported catalysts with little less than 1 wt.% Pt showed comparable activities in HDS of DBT and diesel oil with the activities of a CoMo/Al_2O_3 [4,5,8]. The higher Pt loading (5 wt.% Pt on ZSM-5), led to the higher thiophene HDS activity over CoMo/Al_2O_3 [10], similarly as in our case with Pt(2)/MSA. These examples refer to the single HDS, while in the present work the HDS proceeded simultaneously with HDN. Thus, the results obtained now confirm that high HDS activities of the Pt/MSA catalysts can also be easily achieved in the presence of nitrogen base such as pyridine.

All promoted Pt–Mo/MSA catalysts showed lower thiophene HDS activities per weight unit than conventional CoMo and NiMo/Al_2O_3 systems (Table 4). On the other hand, they exhibited substantially higher hydrogenation efficiency, provided the rate constants k_{PY} are considered, and also, because of a very strong promotion in the C–N bond hydrogenolysis, several times higher overall A(HDN) activities. The conventional CoMo and NiMo/Al_2O_3 catalysts are first of all optimized for maximum HDS performance, their HDN activity and HDN/HDS selectivity is thus lower in comparison to Pt/MSA and Pt–Mo/MSA.

4. Conclusions

The MSA gave Pt/MSA and Pt–Mo/MSA sulfide catalysts active in HDS of thiophene and HDN of pyridine. The addition of Pt to sulfided Mo/MSA led to a marked increase of activities in both reactions. The increment of the activity of the promoted catalysts was significant up to about 0.5 wt.% Pt and lower above this loading. The promotional effect of Pt was very strong in HDN and only weak in HDS. Based on the results of TPR, it can be stated that Pt addition increased substantially reducibility of the MoS_2 phase which reflected in higher activity of the promoted catalysts. The monometallic Pt/MSA sulfide catalysts with 1.3 and 2 wt.% Pt were more active in HDS than the promoted Pt–Mo/MSA catalysts and, at the same time, comparable to the weight equivalents of CoMo and NiMo/Al_2O_3 catalysts. The high HDS activity of Pt/MSA catalysts is most probably given by higher acidity of support and the type of the active sites involved, associated with sulfided Pt phase. The HDS activity of the Pt/MSA catalyst was about five times higher than that of Pt/Al_2O_3. Substitution of Al_2O_3 by acidic MSA in the promoted Pt–Mo catalysts had smaller, but still significant effect. The HDS activity of Pt(0.5)Mo/MSA catalyst normalized to the same amount of metals was still by 25% higher over that of its alumina-supported counterpart.

The parallelism in activities in thiophene HDS and pyridine HYD suggests that these reactions proceed on the same type of sites of Pt/MSA and majority of the Pt–Mo/MSA catalysts, most likely present on sulfided surfaces of Pt and MoS_2 phases. On the other hand, different dependences for the C–N bond hydrogenolysis speak for the different sites involved, rather related to their metallic character, which could be residual metallic Pt fraction and sites created by deeper sulfur abstraction from MoS_2 in the presence of Pt.

Acknowledgement

The financial support of the Czech Science Foundation (grant 104/06/0870) is gratefully acknowledged. The authors thank H. Šnajdaufová (ICPF) for texture measurement and S. Matějková (IOCB) for carbon and nitrogen analyses of the spent catalysts.

References

[1] T.A. Pecoraro, R.R. Chianelli, J. Catal. 67 (1981) 430.
[2] J.P.R. Vissers, C.K. Groot, E.M. van Oers, V.H.J. de Beer, R. Prins, Bull. Soc. Chim. Belg. 93 (1984) 813.
[3] S. Eijsbouts, V.H.J. de Beer, R. Prins, J. Catal. 109 (1988) 217.
[4] W.R.A.M. Robinson, J.A.R. van Veen, V.H.J. de Beer, R.A. van Santen, Fuel Process. Technol 61 (1999) 89.
[5] W.R.A.M. Robinson, J.A.R. van Veen, V.H.J. de Beer, R.A. van Santen, Fuel Process. Technol. 61 (1999) 103.
[6] H.R. Reinhoudt, R. Troost, S. van Schalkwijk, A.D. van Langeveld, S.T. Sie, J.A.R. van Veen, J.A. Moulijn, Fuel Process. Technol. 61 (1999) 117.
[7] A. Niquille-Röthlisberger, R. Prins, Catal. Today 123 (2007) 198.
[8] R. Navarro, B. Pawelec, J.L.G. Fierro, P.T. Vasudevan, J.F. Cambra, P.L. Arias, Appl. Catal. A 137 (1996) 269.
[9] R. Navarro, B. Pawelec, J.L.G. Fierro, P.T. Vasudevan, Appl. Catal. A 148 (1996) 23.
[10] M. Sugioka, F. Sado, T. Kurosaka, X. Wang, Catal. Today 45 (1998) 327.
[11] Z. Vít, J. Cinibulk, D. Gulková, Appl. Catal. A 272 (2004) 99.
[12] Z. Vít, D. Gulková, L. Kaluža, M. Zdražil, J. Catal. 232 (2005) 447.
[13] Y. Kanda, T. Aizawa, T. Kobayashi, Y. Uemichi, S. Namba, M. Sugioka, Appl. Catal. B: Environ. 77 (2007) 117.
[14] E. Peeters, C. Geantet, J.L. Zotin, M. Breysse, M. Vrinat, Stud. Surf. Sci. Catal. 130 (2000) 2837.
[15] J. Blanchard, M. Breysse, K. Fajerwerg, C. Louis, C.-E. Hédoire, A. Sampieri, S. Zeng, G. Pérot, H. Nie, D. Li, Stud. Surf. Sci. Catal. 158 (2005) 1517.
[16] J. Wang, W.-Z. Li, G. Pérot, J.L. Lemberton, C.-Y. Yu, C. Thomas, Y.-Z. Zhang, Stud. Surf. Sci. Catal. 112 (1997) 171.
[17] Z. Paál, T. Koltai, K. Matusek, J.M. Manoli, C. Potvin, M. Muhler, U. Wild, P. Tétényi, Phys. Chem. Chem. Phys. 3 (2001) 1535.
[18] M.C. Carrión, B.R. Manzano, F.A. Jalón, P. Maireles-Torres, E. Rodríguez-Castellón, A. Jiménez-López, J. Mol. Catal. A 252 (2006) 31.
[19] M.H. Pinzón, A. Centeno, S.A. Giraldo, Appl. Catal. A 302 (2006) 118.
[20] S. Pessayre, C. Geantet, R. Bacaud, M. Vrinat, T.S. N'Guyen, Y. Soldo, J.L. Hazemann, M. Breysse, Ind. Eng. Chem. Res. 46 (2007) 3877.
[21] M. Breysse, G. Djega-Mariadassou, S. Pessayre, C. Geantet, M. Vrinat, G. Pérot, M. Lemaire, Catal. Today 84 (2003) 129.
[22] T.J. Paskach, S.J. Hilsenbeck, R.K. Thompson, R.E. McCarley, G.L. Schrader, J. Alloys Compd. 311 (2000) 169.
[23] T.I. Korányi, Z. Vít, D.G. Poduval, R. Ryoo, H.S. Kim, E.J.M. Hensen, J. Catal. 253 (2008) 119.
[24] Z. Vít, O. Šolcová, Micropor. Mesopor. Mater. 96 (2006) 197.
[25] D. Gulková, Z. Vít, Stud. Surf. Sci. Catal. 162 (2006) 489.
[26] Z. Vít, D. Gulková, L. Kaluža, M. Zdražil, React. Kinet. Catal. Lett. 83 (2) (2004) 237.
[27] J. Cinibulk, Z. Vít, Appl. Catal. A 180 (1999) 15.
[28] J.R. Anderson, K.C. Pratt, Introduction to Characterization and Testing of Catalysts, Academic Press (Harcourt Brace Jovanovish, Publishers), New York, 1985, p. 64.
[29] Y. Konishi, M. Ichikawa, W.M.H. Sachtler, J. Phys. Chem. 91 (1987) 6286.
[30] Y. Yoshimura, M. Toba, T. Matsui, M. Harada, Y. Ichihashi, K.K. Bando, H. Yasuda, H. Ishihara, Y. Morita, T. Kameoka, Appl. Catal. A 322 (2007) 152.
[31] J. Cinibulk, D. Gulková, Y. Yoshimura, Z. Vít, Appl. Catal. A 255 (2003) 321.
[32] T. Matsuda, F. Uchijima, H. Sakagami, N. Takahashi, Phys. Chem. Chem. Phys. 3 (2001) 4430.

[33] T. Komatsu, W.K. Hall, J. Phys. Chem. 95 (1991) 9966.
[34] T. Komatsu, W.K. Hall, J. Phys. Chem. 96 (1992) 8131.
[35] A. Blackburn, P.A. Sermon, J. Chem. Technol. Biotechnol. 33A (1983) 120.
[36] M.F. Williams, B. Fonté, C. Sievers, A. Abraham, J.A. van Bokhoven, A. Jentys, J.A.R. van Veen, J.A. Lercher, J. Catal. 251 (2007) 485.
[37] M.D. Appay, J.M. Manoli, C. Potvin, M. Muhler, U. Wild, O. Pozdnyakova, Z. Paál, J. Catal. 222 (2004) 419.
[38] T. Matsui, M. Harada, Y. Ichihashi, K.K. Bando, N. Matsubayashi, M. Toba, Y. Yoshimura, Appl. Catal. A 286 (2005) 249.
[39] P.J. Mangnus, A. Riezebos, A.D. van Langeveld, J.A. Moulijn, J. Catal. 151 (1995) 178.
[40] V.G. Baldovino-Medrano, S.A. Giraldo, A. Centeno, Fuel 87 (2008) 1917.
[41] B. Pawelec, R. Navarro, J.L.G. Fierro, J.F. Cambra, F. Zugazaga, M.B. Güemez, P.L. Arias, Fuel 76 (1) (1997) 61.